

Journal of Climate Change, Vol. 2, No. 2 (2016), pp. 25–34. DOI 10.3233/JCC-160015

Simulations of Heavy Rainfall from a Tropical Cyclone in Coastal Regions of Vietnam under the Global Warming

Lap Quoc Tran and Kenji Taniguchi*

Faculty of Environmental Design, Kanazawa University, Kanazawa, Japan ⊠ taniguti@se.kanazawa-u.ac.jp

Received May 15, 2016; revised and accepted June 17, 2016

Abstract: The central regions of Vietnam often receive heavy rainfall by tropical cyclones in the Western Pacific. A tropical cyclone with strong winds inflicts direct damage to infrastructure, causing losses to both the economy and human life. Heavy rains from a tropical cyclone also cause substantial destruction. Furthermore, because of global warming, the intensity of rainfall is expected to increase in the future. In this study, a record of heavy rainfall event in the central region of Vietnam from Tropical Cyclone Lekima, which hit Vietnam in 2007, was simulated by a Weather Research and Forecast model (WRF), using an ensemble simulation method. Rainfall variability in future climate scenarios was investigated using numerical simulations based on pseudo global warming (PGW) conditions, constructed using third-phase results of Coupled Model Intercomparison Project multi-model global warming experiments. Under certain future climate scenarios, the intensity of rainfall from Tropical Cyclone Lekima would have been heavier than in the present climate. The simulation results show that maximum six-hourly and total precipitation would increase significantly in the future. The spatial distribution of heavy rain from Tropical Cyclone Lekima would tend to shift from North to Southwest Vietnam. Simulation results suggest that global warming may correlate with a significant increase in rainfall.

Keywords: Climate change, Numerical simulation, Heavy rainfall, Ensemble simulation.

Introduction

Tropical cyclones (TCs) with strong winds cause economic damage and loss of human life (Blake et al. 2007; Elsberry 2002; Rappaport 2000; Sheets 1990). Heavy rain during tropical cyclones is also a destructive factor, which occurs as the TC makes landfall (Larson et al., 2005). Studies of past tropical cyclones based on observations show that variations in the frequency of TCs is ambiguous, but a clear increase has been recognized in the number of strong hurricanes in the late 20th century. Future variability in storms will be greater and a significant increase in economic losses is expected (Pielke et al., 2005; Webster et al., 2005). In future climate conditions, studies of global TC frequency show decreasing trends (Emanuel et al.,

2008; Kim et al., 2014; Murakami et al., 2011; Oouchi et al., 2006). Variations in specific regions have also been investigated: there is an increasing trend of TC genesis in the central North Pacific, while a decreasing trend is observed in western parts (Yokoi and Takayabu, 2009). For rainfall amount, Hasegawa et al. (2005) showed 8.4% increase in rainfall associated with tropical cyclones in the late 21st century around the Western North Pacific. Chiang et al. (2011) showed an increase in annual maximum tropical cyclone rainfall in Taiwan island from 322 mm (1960–2008) to 371 mm (2010–2099).

There have been a large number of studies assessing the effects of global warming. Simulation outputs from coupled atmosphere-ocean global climate models (AOGCMs) are often used in studies of future climate. However, the spatial resolution of AOGCMs is generally several hundreds of kilometres. Thus, AOGCM resolution is too coarse to investigate detailed changes in extreme heavy rainfall events. Higherresolution climatic conditions can be simulated by a dynamic downscaling (DDS) technique using a physical model. Sato et al. (2007) used a DDS method to model future changes of water resources in Mongolia. They calculated a 10-year mean difference between 20th century and future climate runs using an AOGCM, and the difference was added to reanalyse data to create a forcing dataset for the DDS. This new forcing dataset is called a pseudo global warming (PGW) condition. A future DDS result using PGW forcing can be compared directly with a present DDS result from reanalysis data. Sato et al. (2007) showed that reproducibility of the current climate in a DDS result with reanalysis data was superior to that of the original AOGCM output. Therefore, DDS results of PGW forcing are expected to effectively reflect the effects of global warming on the current climate.

Located along the east coast of the Indochina Peninsula with a substantial latitudinal extent on the northwest Pacific Ocean, Vietnam is one of the countries most strongly affected by TCs. According to Garcia (2002), Vietnam is struck by an average of four to six tropical cylones per year. Nguyen-Thi et al. (2012) investigated the seasonal and regional characteristics of the climatological rainfall associated with TCs in the coastal region of Vietnam. The results showed that TC rainfall varies from 0 to ~25% of total rainfall, in which the mid-central region of Vietnam receives the maximum value and also has the highest TC frequency.

In the current study, the pseudo global warming (PGW) downscaling approach (Sato et al., 2007) was applied to investigate the future variations in heavy rainfall caused by tropical cyclones in the coastal regions of Vietnam. For this purpose, we selected Tropical Cyclone Lekima from 2007 and made hindcast and PGW simulations to investigate the changes in rainfall. In next Section, an overview of the dataset and design of the dynamic downscaling (DDS) with PGW forcing data are provided. In subsequent Section, hindcast simulations of heavy rainfall caused by the Lekima are discussed. In penultimate Section, simulations of rainfall changes in future climate scenarios from the DDS are investigated with PGW conditions. Finally, a summary is given in the last Section.

Data and Methodology

Data

JRA-55

The Japanese 55-year reanalysis product (JRA-55) by the Japan Meteorological Agency (JMA) was used for simulations of the Lekima. JRA-55 is produced by a system based on the low-resolution (TL319) version of JMA's operational data assimilation system, which has been extensively improved since the previous reanalysis (JRA-25). The atmospheric component of JRA-55 is based on the incremental four-dimensional variational method. Newly available and improved past observations are used for JRA-55. Major problems in JRA-25 (cold bias in the lower stratosphere and dry bias in the Amazon) have been resolved in JRA-55; therefore, the temporal consistency of temperature is improved. Further details are available in Kobayashi et al. (2015).

CMIP3 Multi-model Dataset

For assessment of future global warming, coordinated numerical experiments have been conducted by many modeling groups using state-of-the-art global coupled climate models under the framework of the Coupled Model Intercomparison Project (CMIP). In this study, we used future climate projections of the third phase of the CMIP (CMIP3; Meehl et al., 2007). Newer climate projections of the fifth phase of CMIP (CMIP5) have been published. Comparison of performances of AOGCMs in CMIP3 and CMIP5 showed that ranges of uncertainty in CMIP3 and CMIP5 were comparable, and their model performances were generally similar (IPCC, 2013). Knutti and Sedláček (2013) showed similarity in projected global temperature and precipitation between CMIP3 and CMIP5 models. Therefore, there are similar uncertainties in both output; thus, the CMIP3 dataset is still useful in climate change studies.

In CMIP3, the scenario used for simulations of the present day climate is known as the 20th Century Climate in Coupled Models (20C3M) (Nakicenovic and Swart, 2000). Future projections were made using several possible emission scenarios. The future climate projections used in this study were AOGCM outputs under the Special Report on Emissions Scenario A1B (Nakicenovic and Swart, 2000). A list of the CMIP3 data and abbreviations of ensemble simulations with PGW forcing are given in Table 1.

CMIP3 ID Ensemble name Institute Country 1 CCCMA T47 PGW 1 Canadian Centre for Climate Modelling and Analysis Canada 2 CCCMA T63 PGW 2 Canadian Centre for Climate Modelling and Analysis Canada 3 CNRM CM3 PGW 3 Meteo-France, Centre Nationale de France RecherchesMeteorologique 4 GISS H PGW 4 NASA/Goddard Institute for Space Studies United States 5 INMCM PGW 5 Institute of Numerical Mathematics Russia 6 MIROC H PGW 6 Center for Climate System Research (the University of Tokyo), National Institute for Environmental Japan Studies, and Frontier Research Center for Global Change 7 MRI CGCM PGW 7 Meteorological Research Institute Japan 8 UKMO HadGEM1 PGW 8 Hadley Centre for Climate Prediction and Research, United Kingdom

Met Office

Table 1: List of the CMIP3 models used for analysis

Sea Surface Temperature (SST)

For SST in the simulations, we used the NOAA Optimum Interpolation 1/4 Degree Daily Sea Surface Temperature Analysis (NOAA OI SST) (Reynolds et al., 2007). The NOAA OI SST dataset has a grid resolution of 0.25° and temporal resolution of one day. The product uses Advanced Very High-Resolution Radiometer infrared satellite SST data. Advanced Microwave Scanning Radiometer SST data were used after June 2002. In situ data from ships and buoys were also used for large-scale adjustment of satellite biases.

Land-surface Conditions

For the land-surface condition in the numerical simulations (volumetric soil moisture, soil temperature, soil type and vegetation type), we used National Centers for Environmental Prediction (NCEP) Final Operational Global Analysis (NCEP FNL) data. NCEP FNL data are produced on a 6-hourly basis by the NCEP global data analysis system from July 1999 to the near present. Data spatial resolution is 1.0° × 1.0° (NCEP, 2000).

Rainfall Data for Verification

As rainfall data for verification of the Lekima results, we used in-situ observation data from seven rain gauge observations in seven provinces in the coastal area of Vietnam. The locations and names of weather stations are shown in Figure 1(a). In Vietnam, weather radar stations over the whole territory are fairly sparse. Hence, to examine the detailed distribution of precipitation in the central region of Vietnam, simulated results were compared with the APHRODITE precipitation dataset (Asian Precipitation - Highly-Resolved Observational Data Integration Towards Evaluation). The APHRODITE dataset Ver.1101R2, with a spatial

resolution of 0.25° for the Monsoon Asia region, was used in this study (Yatagai et al., 2012).

Overview of Tropical Cyclone Lekima

A tropical depression formed in the South China Sea at 06:00 UTC 30 September 2007 at approximately 115°E/14.7°N. Initially, it moved in a north-west direction towards Hainan Island, whilst simultaneously intensifying before becoming a tropical storm named Lekima at 12:00 UTC, where it continued in a northwest direction. Then, it slowly changed direction to westnorth-west and continued getting stronger. At 00:00 UTC 02 October, it developed into a typhoon category and continued its trajectory toward the Vietnam coast and hit the land at 12:00 UTC 03 October at 106.5°E/17.9°N. The most dangerous aspects of storm Lekima were the very strong winds, coupled with heavy rainfall and flooding following its path. Total rainfall exceeded 400 mm at many observation sites, and the maximum value was 660 mm in Thua Thin Hue Province.

Pseudo Global Warming Conditions

Control simulations of the Lekima (CTL) were performed with initial and boundary conditions prepared from JRA-55, NCEP FNL and NOAA 0.25 interpolated OI SST. In addition to CTL, we performed simulations with PGW forcing prepared using different CMIP3 data. PGW conditions of the Lekima were calculated from future and present climate conditions. The future weather conditions were obtained from the 10-year monthly mean from 2091 to 2100. Present climatic conditions were obtained from the 10-year monthly mean from 1991 to 2000 in 20C3M. Then, anomalies of global warming were calculated as the difference

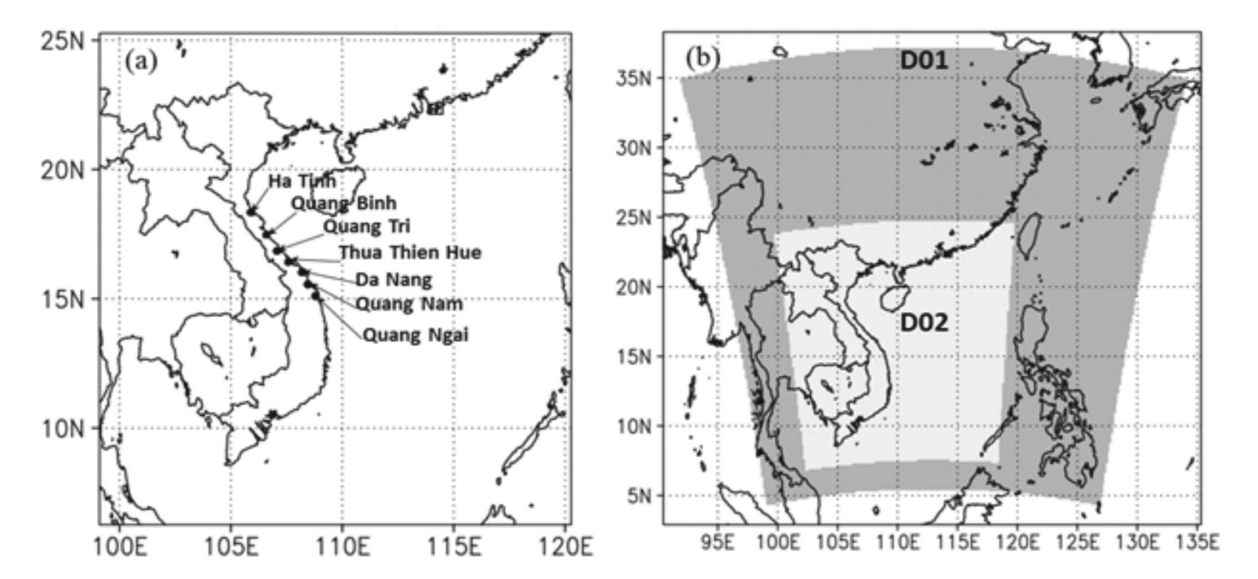


Figure 1: (a) Location of seven rain gauge observations and (b) target domains of downscaling in the weather research and forecasting (WRF) model. Areas indicated by dark and light shading are D01 and D02, respectively. The spatial resolutions are 30 km and 10 km for D01 and D02, respectively.

between future and present climatic conditions and added to JRA-55. Thus, a set of PGW conditions was constructed for the wind, atmospheric temperature, geopotential height, surface pressure and specific humidity. For relative humidity, the original values in JRA-55 were retained in the PGW conditions, and specific humidity in these conditions was defined from the relative humidity and the modified atmospheric temperature of the future climate. To prepare SST for the PGW condition, the SST anomaly obtained from future and present climate conditions in the CIMP3 output was added to the NOAA SST.

Design of Numerical Simulations

In this study, weather research and forecasting model (WRF) version 3.6.1 was adopted for the CTL and PGW simulations. A two-way nesting grid system was used, as shown in Figure 1 (b). The coarsest domain (D01) had a 30-km horizontal resolution and the higher resolution domain D02 had a 10-km horizontal resolution.

Ensemble simulations with different initial conditions were performed for the CTL and each PGW condition. At first, the lagged average forecast (LAF) method (Hoffman and Kalnay, 1983) was used to obtain three different conditions X_1 , X_2 , and X_3 (Figure 2). In LAF, multiple simulations with different initial times were performed. The three simulations were set up with 6-hour lags, so that the simulations began at 00:00 UTC, 06:00 UTC and 12:00 UTC on 30 September. From three ensemble members, two perturbation states (ΔX_2 and ΔX_3) were produced, as follows:

$$\Delta X_2 = X_2 - X_1$$

$$\Delta X_3 = X_3 - X_1$$

Then, a new state was made from the following equation:

$$X_n = X_1 + \alpha \times \Delta X_2 + \beta \times \Delta X_3$$

Here, α and β are scale factors of ΔX_2 and ΔX_3 . Sixteen new ensemble members were prepared at 00:00 UTC on 01 October. In total, 19 simulations were made (Figure 2) until 18 UTC 04 October. Pairs of the scale factors are listed in Table 2. Ensemble simulations enable stochastic analysis of differences between CTL

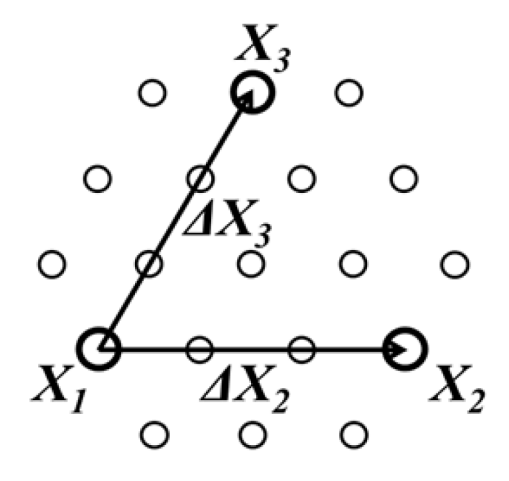


Figure 2: Schematic view of ensemble member preparation. Large open circles are the base states $(X_1, X_2, \text{ and } X_3)$ made by the LAF method. Small open circles are newly prepared ensemble states.

and PGW runs. Therefore, it could be determined whether differences were attributable to the effects of global warming or chaotic behaviours in the numerical weather model.

Kain-Fritsch cumulus parameterization (Kain, 2004), and the microphysics parameterization schemes of Lin et al. (1983) were used in this study. Physical processes of the surface layer, land surface scheme, and planetary boundary layer scheme have been computed by MM5 similarity based on Monin-Obukhov with Carslon-

Boland viscous sub-layer, Noah Land Surface model (Chen et al., 2001), and Yonsei University scheme (Hong et al., 2006). For long wave radiation, we used the RRTM scheme (Mlawer et al., 1997), and for shortwave radiation we used the Goddard shortwave scheme (Chou and Suarez, 1994). For D01, a spectral nudging method was used for atmospheric temperature, zonal wind, meridional wind, and geopotential height every six hours at altitudes above 6–7 km. Model settings are given in Table 3.

Table 2: Pairs of the scale factors (α and β) in $X_n = X_1 + \alpha \times \Delta X_2 + \beta \times \Delta X_3$

(α, β)	(α, β)	(α, β)	(α, β)
(-1/3, 1/3)	(0, 2/3)	(1/3, 2/3)	(2/3, 1/3)
(-1/3, 2/3)	(1/3, -1/3)	(1/3, 1)	(2/3, 2/3)
(-1/3, 1)	(1/3, 0)	(2/3, -1/3)	(1, -1/3)
(0, 1/3)	(1/3, 1/3)	(2/3, 0)	(1, 1/3)

^{*}The original three states $(X_1, X_2, \text{ and } X_3)$ are not included.

Table 3: WRF settings

Version of model	V 3.6.1		
Number of domain	Two		
Horizontal grid distance	30 km (coarse domain); 10 km (fine domain)		
Cloud microphysics	Lin et al. method		
Cumulus parameterization	Kain-Fritsch scheme cumulus parameterization		
Long wave radiation	RRTM scheme Rapid Radiative Transfer Model		
Short wave radiation Surface layer	Goddard shortwave MM5 similarity		
Land surface scheme	Noah Land Surface model		
Planetary boundary layer scheme	Yonsei University scheme		
Setting of spectral nudging	A spectral nudging method was used for atmospheric temperature, zonal wind, meridional wind, and geopotential height every six hours, at altitudes above 6-7 km.		

Results of Control Runs (CTL)

In CTL, Lekima hit land on the coast of Vietnam at 12:00 UTC 3 October at 106.5°E/17.9°N. Figure 3 shows the simulation results of precipitation. Figure 3 (a) indicates that total rainfall in the coastal areas of Vietnam from 06:00 UTC 01 October to 06:00 UTC 04 October 2007 tend to be underestimated in CTL. Especially in Quang Tri, Da Nang and Quang Nam, the results of average ensemble members are smaller than observation data.

Figures 3 (b) and (c) show the spatial distribution of total precipitation of the APHRODITE dataset, and ensemble-mean results of CTL. Similar to the result of APHRODITE, heavy rainfall spreads from the north to the south, and concentrates mainly along the central region of Vietnam. The total rainfall ranges from 200 mm to 300 mm along the coastal area in central parts of Vietnam. However, APHRODITE rainfall ranges from 100 mm to 150 mm along the coastal area, so the quantity of precipitation is larger in CTL than in APHRODITE.

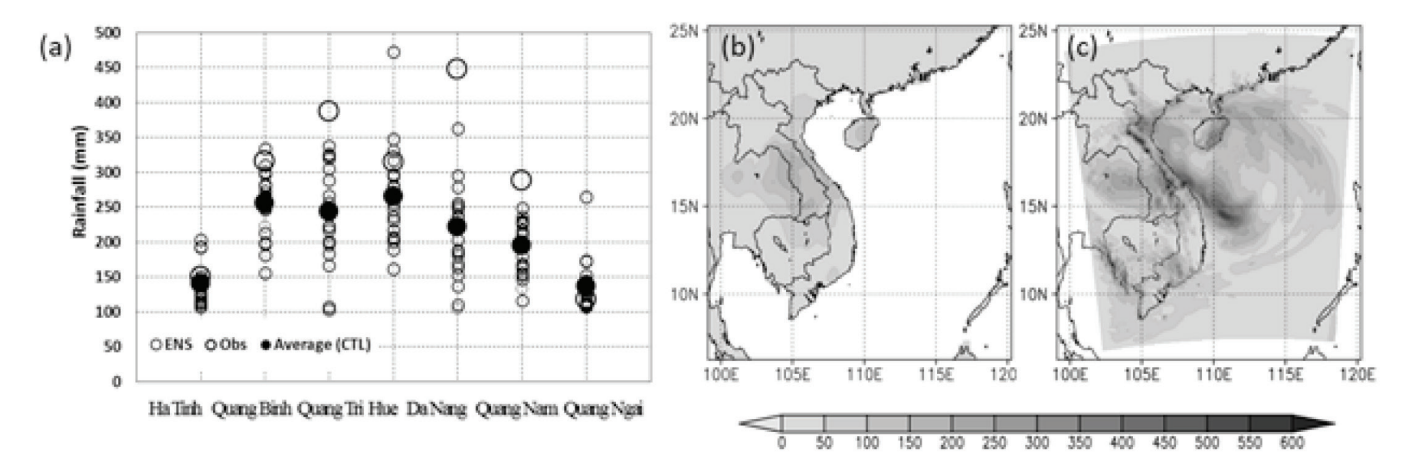


Figure 3: (a) Rainfall at seven rain gauge stations. Large black solid circles and small open circles are average rainfall simulation results and rainfall simulation results of each ensemble member, respectively. Large open circles are the observation values from seven rain gauge stations in the central part of Vietnam. Vertical axis is rainfall (mm). (b) and (c) Spatial distribution of rainfall from APHRODITE data and average total rainfall from nineteen ensemble members from 06 UTC 01 October to 06 UTC 04 October 2007 in D02, respectively. Colour bar shows rainfall (mm).

Results of Pseudo Global Warming Experiments

Maximum Six-hourly Rainfall

The maximum six-hourly rainfall in ensemble simulations is compared between CTL and PGW experiments (Figure 4 (a)). Ensemble mean values in all PGW runs are larger than from the CTL. The results of maximum six-hourly rainfall increase from 27% to 78% in all PGW experiments. The highest increase in maximum six-hourly precipitation (the average from nineteen ensemble members) is 413.75 mm at PGW_6, followed by PGW_3, PGW_2, and PGW_4 with 370.01 mm, 343.69 mm and 329.18 mm, respectively.

The lowest increase in maximum six-hourly rainfall is 61.69 mm in run PGW_1. Figure 4 (b) presents probability density curves of maximum six-hourly rainfall simulated by PGW experiments and the CTL runs. It is clear that there is a significant increase in the amount of rainfall in all PGW runs, and the results indicate that some extreme heavy rainfall events will occur only in future climate scenarios.

Figure 5 displays the spatial distribution of maximum six-hourly rainfall from 06:00 UTC 01 October to 18:00 UTC 04 October between PGW experiments and the CTL runs. The heavy rain areas extend from the north to the south of the central region of Vietnam. Especially in PGW 6, PGW 7, PGW 2 and PGW 3, the spatial

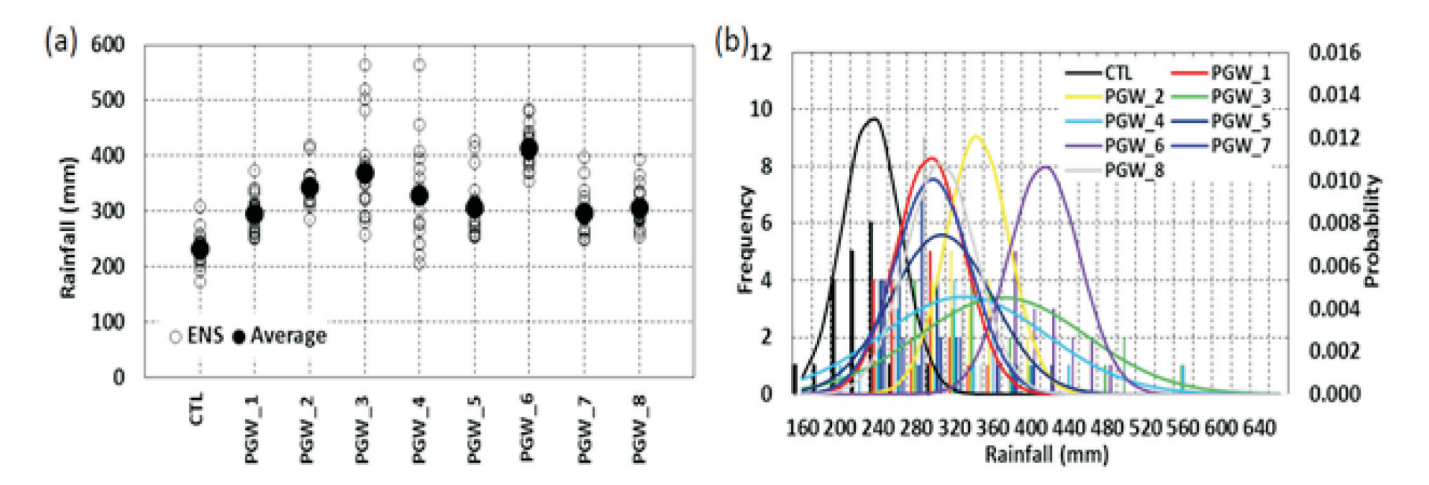


Figure 4: (a) Maximum six-hourly rainfall for each simulation and ensemble mean result. (b) Frequency distributions and probability density curves of maximum six-hour rainfall by PGW experiments and CTL runs.

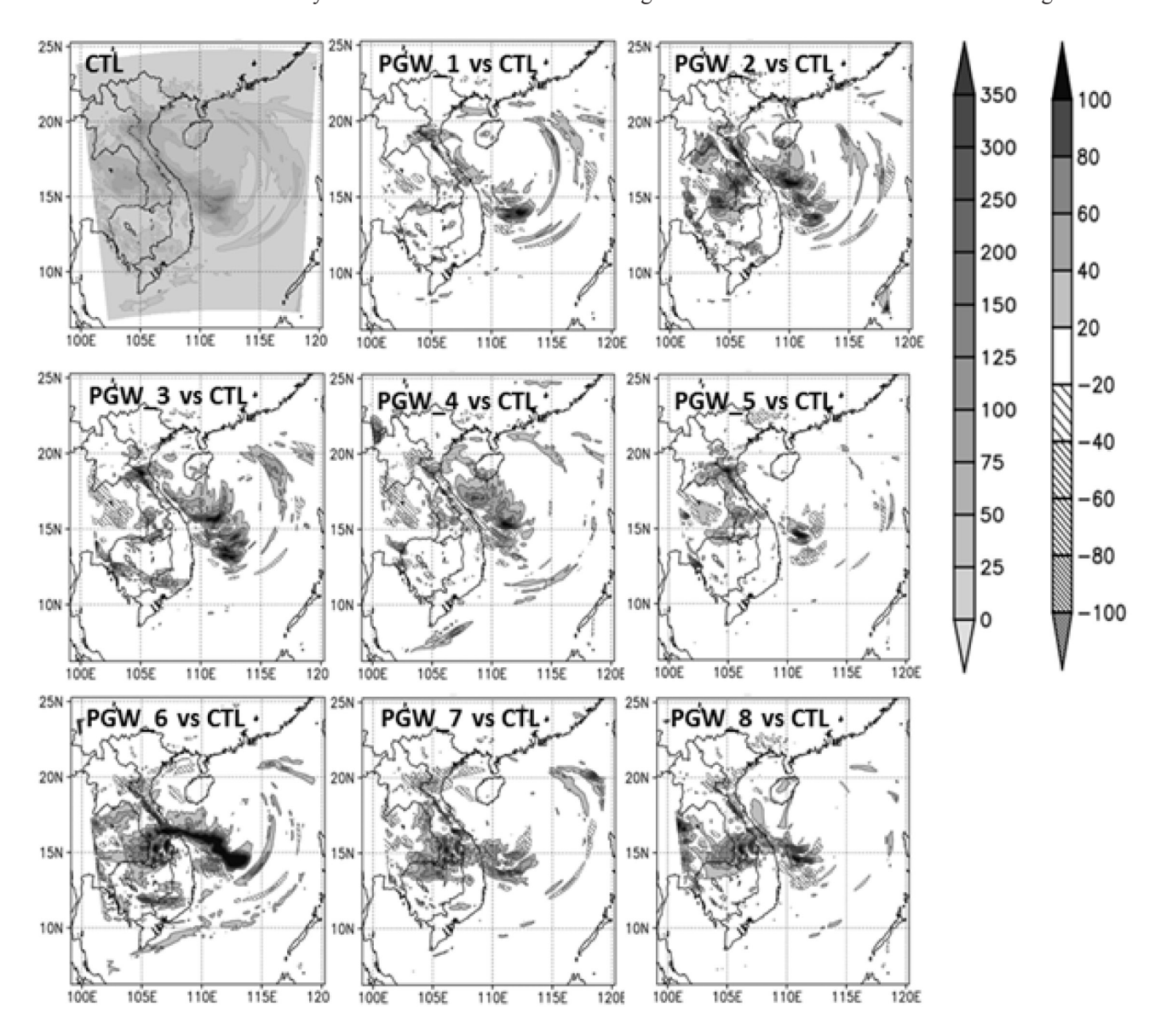


Figure 5: Ensemble-mean maximum six-hourly rainfall of CTL and the difference in ensemble-mean maximum six-hourly rainfall between PGW and CTL runs. Left- and right-hand colour bars are for the maximum six-hourly rainfall and the differences between PGW and CTL (mm), respectively.

distribution of heavy rain occurs over a vast area and shifts from north to south and southwest, and expands from Vietnam to Laos and Thailand.

Variations in Total Rainfall

Figure 6 shows the maximum total rainfall values and their probability density curves from 06:00 UTC 01 October to 06:00 UTC 04 October in PGW and CTL runs. All PGW runs show an increase in the intensity of total rainfall (Figure 6 (a)). The ensemble mean maximum total rainfall of CTL is ~656.38 mm. For PGW_6, PGW_8, PGW_2 and PGW_4, the average total rainfall is higher than 1000 mm, whereas the

simulated results from PGW_1, PGW_5 and PGW_4 experiments are 921.45 mm, 903.63 mm and 746.02 mm, respectively. Therefore, for all PGW experiments, total rainfall from tropical cyclones will increase in the future. Figure 6 (b) shows clear shifts in the probability density curves. These results indicate that in the far future, a tropical cyclone similar to Lekima would frequently cause heavier rainfall than in the present climatic conditions.

Figure 7 illustrates the difference in the spatial distribution of total rainfall between PGW experiments and CTL runs. For PGW_6, PGW_8 and PGW_2, precipitation increases significantly and spreads over

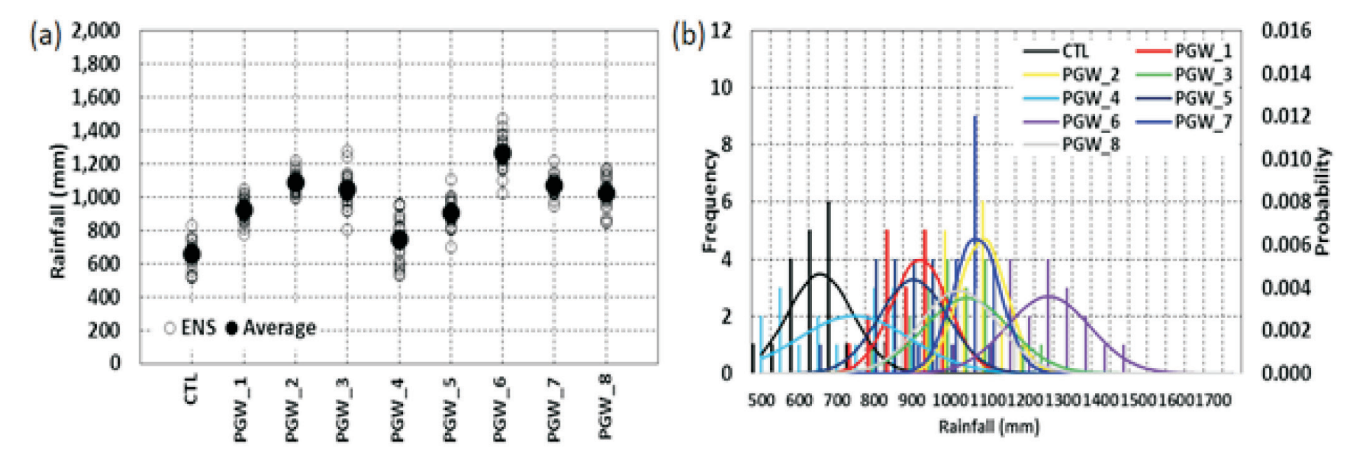


Figure 6: (a) Maximum total rainfall (from 06UTC 01 October to 06UTC 04 October) for each simulation and ensemble mean result. (b) Frequency distributions and probability density curves of maximum total rainfall by PGW experiments and CTL runs.

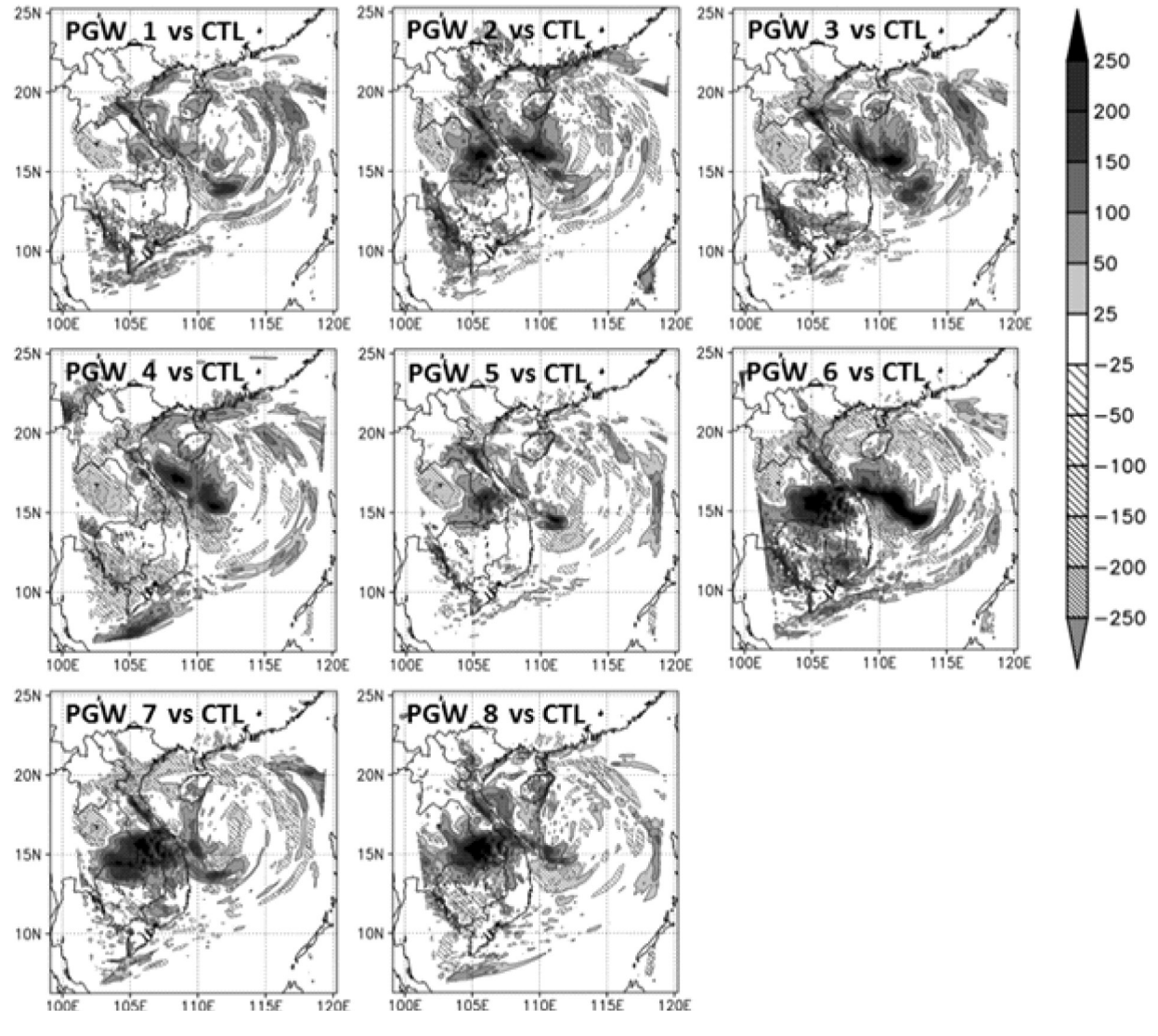


Figure 7: Difference of ensemble-mean total rainfall between PGW experiments and CTL runs. Colour bar shows the difference in rainfall (mm).

a wide area of central regions in Vietnam. Torrential rain continues inland over Laos and into Thailand after passing through Vietnam. However, in PGW_7 and PGW_8, the rainfall decreases in the north and increases in the south of central areas, whereas the spatial distribution results from experiment PGW_4 show a downward trend in heavy rainfall inland.

Overall, rainfall due to tropical cyclones in the central regions of Vietnam increases in intensity in the future when using PGW experiments. The future spatial distribution of rainfall tends to shift from north to south, expanding into southwest regions and passing over Laos and into Thailand. The simulation results of heavy rainfall from experiment PGW_6 show the largest increase in rainfall intensity in the future.

Summary

This study aims to perform a hindcast of heavy rainfall caused by Tropical Cyclone Lekima on the Vietnam Central Coast from 30 September to 04 October 2007, and investigate the variations in torrential rain under global warming climate conditions using the PGW method. In the hindcast and the simulations using the PGW method, 19 ensemble members were prepared based on the LAF method. In the hindcast (CTL), the torrential rains were underestimated in some regions when compared to observation data, the rainfall distribution for the Lekima shifted from north to south, and the location and intensity differed among ensemble members. In the future simulations, the heavy rainfall regions moved to the southwest to affect central areas of Vietnam, Laos and Thailand. The fluctuation of sixhourly and total rainfall was wide among ensemble members of CTL runs and PGW experiments. Torrential rains may occur over short periods and larger areas in future climate conditions. The spatial distribution of precipitation in PGW runs was larger than in the CTL runs. Probability density curves of the maximum total and six-hourly precipitation showed clear differences between current and future climate conditions. The results indicate that tropical cyclones similar to the Lekima can produce extremely heavy rainfall that would not be expected in the current climate. This is because, under the global warming, saturated water vapour will increase and the warmer SST will provide more water vapour. For detailed mechanism, further analysis is needed.

Only one tropical cyclone was examined in this study and the conclusions drawn about variations in heavy rainfall due to future global warming may include some uncertainty. It is thought that the results of this study are the first step in evaluating heavy rainfall from tropical cyclones in the future, and investigation of other tropical cyclones, as well as the use of additional AOGCMs and climate change scenarios, will be indispensable for assessing changes in heavy rainfall due to climate change.

Acknowledgements

The authors are grateful for the use of CMIP3 products archived and published by the Program for Climate Model Diagnosis and Intercomparison (PCMDI) and to all research institutes contributing to this activity. We would like to thank the Vietnam National Hydrometeorology Center for providing the rainfall data sets from seven rain gauge stations in the central region. Japanese 55-Year reanalysis data were provided by the Japan Meteorological Agency (JMA) and the Central Research Institute of Electric Power Industry (CRIEPI). The best-track data for Tropical Cyclone Lekima were provided by the Joint Typhoon Warning Center (JTWC). The authors would like to thank anonymous reviewers for their helpful comments and suggestions for improving the quality of the manuscript.

References

Blake, E.S., Rappaport, E.N. and Landsea, C.W., 2007. The deadliest, costliest, and most intense United States tropical cyclones from 1851 to 2006 (and other frequently requested hurricane facts). NOAA Tech. Memo. NWS TPC-5 [Available online at www.nhc.noaa.gov/pdf/NWS-TPC-5.pdf].

Chen, F. and Dudhia, J., 2001. Coupling an advanced land-surface/hydrology model with the Penn State/NCAR MM5 modeling system. Part I: Model description and implementation. *Mon. Wea. Rev.*, **129:** 569–585.

Chiang, S.-H. and Chang, K.-T., 2011. The potential impact of climate change on typhoon-triggered landslides in Taiwan, 2010-2099. *Geomorphology*, **133**: 143-151. doi:10.1016/j. geomorph.2010 .12.028.

Chou, M.-D. and Suarez, M.J., 1994. An efficient thermal infrared radiation parameterization for use in general circulation models. NASA Tech. Memo. 104606 3.

- Elsberry, R.L., 2002. Predicting hurricane landfall precipitation: Optimistic and pessimistic views from the symposium on precipitation extremes. *Bull. Amer. Meteor. Soc.*, **83:** 1333–1339.
- Emanuel, K., Sundararajan, R. and Williams, J., 2008. Hurricanes and global warming: Results from downscaling IPCC AR4 simulations. *Bull Am Meteor Soc*, **89**: 347–367.
- Garcia, L., 2002. Overview of early warning systems for hydro-meteorological hazards in selected countries in Southeast Asia. Asian Disaster Preparedness Center, Thailand.
- Hasegawa, A. and Emori, S., 2005. Tropical cyclones and associated precipitation over the western North Pacific: T106 atmospheric GCM simulation for present-day and doubled CO₂ climates. *SOLA*, **1:** 145–148. doi:10.2151/sola.2005-038.
- Hoffman, R.N. and Kalnay, E., 1983. Lagged average forecasting, and alternative to Monte Carlo forecasting. *Tellus A*, **35:** 100–118.
- Hong, S.-Y., Noh, Y. and Dudhia, J., 2006. A new vertical diffusion package with explicit treatment of entrainment processes. *Mon. Wea. Rev.*, 134: 2318–2341.
- IPCC, 2013. Climate Change 2013: The Physical Science Basis. Cambridge University Press.
- Kain, J.S., 2004. The Kain-Fritsch Convective Parameterization: An Update. *Journal of Applied Meteorology*, 43(1): 170-181.
- Kim, H.-S., Vecchi, G.A., Knutson, T.R., Anderson, W.G., Delworth, T.L., Rosati, A., Zeng, F. and Zhao, M., 2014. Tropical cyclone simulation and response to CO₂ doubling in the GFDL CM2.5 high-resolution coupled climate model. *J. Climate*, 27: 8034–8054.
- Kobayashi, S., Ota, Y., Harada, Y., Ebita, A., Moriya, M., Onoda, H., Onogi, K., Kamahori, H., Kobayashi, C., Endo, H., Miyaoka, K. and Takahashi, K., 2015. The JRA-55 Reanalysis: General specifications and basic characteristics. *J. Meteor. Soc. Japan*, **93:** 5–48.
- Knutti, R. and Sedláček, J., 2013. Robustness and uncertainties in the new CMIP5 climate model projections. *Nat. Climate Change*, **3:** 369–373.
- Larson, J., Zhou, Y. and Higgins, R.W., 2005. Characteristics of landfalling tropical cyclones in the United States and Mexico: Climatology and interannual variability. *J. Climate*, **18:** 1247–1262.
- Lin, Y.-L., Farley, R.D. and Orville, H.D., 1983. Bulk parameterization of the snow field in a cloud model. *J. Climate Appl. Meteor.*, **22:** 1065–1092.
- Meehl, G., Covey, C., Delworth, T., Latif, M., McAvaney, B., Mitchell, J., Stouffer, R. and Taylor, K., 2007. The WCRP CMIP3 multimodel dataset. *Bull. Am. Meteorol. Soc*, **88**: 1383–1394.
- Mlawer, E.J., Taubman, S.J., Brown, P.D., Iacono, M.J. and Clough, S.A., 1997. Radiative transfer for inhomogeneous

- atmosphere: RRTM, a validated correlated-k model for the longwave. J. Geophys. Res, **102(D14)**: 16663–16682.
- Murakami, H., Wang, B. and Kitoh, A., 2011. Future changes of western north pacific typhoons: Projections by a 20-km-mesh global atmospheric model. *J. Climate*, **24**: 1154–1169.
- Nakicenovic, N. and Swart, R., 2000. IPCC special report. Emission Scenario. Cambridge University Press.
- NCEP, 2000. NCEP FNL Operational model global tropospheric analyses, continuing from July 1999. Research Data Archive at the National Center for Atmospheric Research, Computational and Information Systems Laboratory. Boulder, CO. [Available at http://dx.doi.org/10.5065/D6M043C6.].
- Nguyen-Thi, H.A., Matsumoto, J., Ngo-Duc, T. and Endo, N., 2012. A climatological study of tropical cyclone rainfall in Vietnam. *SOLA*, **8:** 41–44.
- Oouchi, K., Yoshimura, J., Yoshimura, H., Mizuta, R., Kusunoki, S. and Noda, A., 2006. Tropical cyclone climatorogy in a global-warming climate as simulated in a 20km-mesh global atmospheric model: Frequency and wind intensity analysis. *J. Meteor. Soc. Japan*, 84: 259–279.
- Pielke Jr., A.R., Landsea, C., Mayfield, M., Laver, J. and Pasch, R., 2005. Hurricanes and global warming. *Bull. Amer. Meteor. Soc.*, **86:** 1571–1575.
- Rappaport, E.N., 2000. Loss of life in the United States associated with recent Atlantic tropical cyclones. *Bull. Amer. Meteor. Soc.*, **81:** 2065–2073.
- Reynolds, R.W., Smith, T.M., Liu, C., Chelton, D.B., Casey, K.S. and Schlax, M.G., 2007. Daily high-resolution blended analysis for sea surface temperature. *J. Climate*, **20:** 5473–5496.
- Sato, T., Kimura, F. and Kitoh, A., 2007. Projection of global warming onto regional precipitation over Mongolia using a regional climate model. *J. Hydrol*, **333**: 144–154.
- Sheets, C.R., 1990. The National Hurricane Center—Past, present, and future. *Wea. Forecasting*, **5:** 185–232.
- Webster, P.J., Holland, G.J., Curry, J.A. and Chang, H.-R., 2005. Changes in tropical cyclone number, duration, and intensity in a warming environment. *Science*, **309**: 1844–1846.
- Yatagai, A., Kamiguchi, K., Arakawa, O., Hamada, A., Yasutomi, N. and Kitoh, A., 2012. APHRODITE: Constructing a long-term Daily Gridded Precipitation Dataset for Asia based on a dense network of rain gauges. *Bull. Am. Meteorol. Soc*, 93: 1401–1415.
- Yokoi, S. and Takayabu, Y.N., 2009. Multi-model projection of global warming impact on tropical cyclone genesis frequency over the western north Pacific. *J. Meteor. Soc. Japan*, **87:** 525–538.